

By acceptance of this article, the publisher or recipient acknowledges the U.S. Government's right to retain a nonexclusive, royalty free license in and to any copyright covering the article

Stress Analysis of Superconducting Magnets for Magnetic Fusion Reactors*

J. E. Akin
Department of Engineering Science and Mechanics
University of Tennessee
Knoxville, Tennessee

W. H. Gray
Fusion Energy Division
Oak Ridge National Laboratory
Oak Ridge, Tennessee

T. V. Baudry
Engineering Division
Oak Ridge National Laboratory
Oak Ridge, Tennessee

MASTER

ABSTRACT

Superconducting devices involve several factors that normally are not encountered in the structural analysis of more common systems. Several of these factors are noted and methods for including them in an analysis are cited. To illustrate the state of the analysis art for superconducting magnets, in magnetic fusion reactors, two specific projects are illustrated. They are the Large Coil Program (LCP) and the Engineering Test Facility (ETF).

INTRODUCTION

As a structure a superconducting magnet must function in an unusual and severe environment. To function as a superconductor it must be maintained at a temperature near 4K, carry large currents in a high peak magnetic field, resist the resulting electromagnetic body forces as well as gravity and thermal stresses, and survive a fast neutron fluence radiation environment. In addition it usually consists of nonhomogeneous composite materials some of which, such as NbTi and Nb3Sn, have unusual structural properties. Many of these difficulties have been overcome. The history of the required developments can be traced through publications such as the semi-annual IEEE Symposiums on Engineering Problems of Fusion Research. A good introduction to the area is given by Moon (1) in the present symposium.

The multi-layered materials are usually smoothed by a law of mixtures as proposed by Sun and Gray (2). However, more advanced computational procedures have been demonstrated by Chang, et al. (3). Of course other difficulties are associated with defining mechanical properties at the temperature of liquid Helium (4.2K). Many of these concepts were utilized in the early studies of small (<1mOD) superconducting magnets. Most were small high field solenoids such as those studied by Gray and Akin (4) and Cain and Gray (5). However, very large solenoids are now being planned for energy storage and their analysis considerations are described by Eyssa, et al. (6) at this symposium.

Here we are interested primarily in the structural analysis of superconducting coils in magnetic fusion reactors. Specifically we will consider the toroidal magnetic field (TF) coils used in existing and proposed tokamak devices. In addition to the usual loading conditions it is very important to include the

*Research sponsored by the Office of Fusion Energy, US Dept. of Energy, under contract W-7405-eng-26 with the Union Carbide Corporation.

DISCLAIMER

This book was prepared as an account of work sponsored by an agency of the United States Government. Neither the United States Government nor any agency thereof, nor any of their employees, makes any warranty, express or implied, or assumes any legal liability or responsibility for the accuracy, completeness, or usefulness of any information, apparatus, product, or process disclosed, or represents that its use would not infringe privately owned rights. Reference herein to any specific commercial product, process, or service by trade name, trademark, manufacturer, or otherwise, does not necessarily constitute or imply its endorsement, recommendation, or favoring by the United States Government or any agency thereof. The views and opinions of authors expressed herein do not necessarily state or reflect those of the United States Government or any agency thereof.

DISTRIBUTION OF THIS DOCUMENT IS UNLIMITED

Handwritten signature or initials.

electromagnetic body forces that are induced in the superconducting coil. This requires the calculation of the magnetic field distributions for the expected loading cases. These cases would include the symmetric normal operating mode as well as nonsymmetric coil fault cases. Various preprocessors have been developed to supply these electromagnetic loading data. A typical example is the TORMAC program (7). A typical coil centering force for the symmetric operating mode would be about $11 \times 10^6 \text{N}$. Large overturning moments also develop in the fault loading case.

THE LARGE COIL PROGRAM

To provide more specific details consider the ORNL Large Coil Program which involves relatively large components. It is a six coil compact torus test stand facility enclosed in a 11m diameter vacuum tank having nitrogen cooled walls. The major structural components include a central bucking post, the six symmetrically placed TF Coils, a spider base structure and a torque ring system. The TF coils are D-shaped with inner bore dimensions of 2.5 x 3.5 m in the horizontal and vertical directions respectively.

A test coil will operate at a peak magnetic field of at least 8.0T at a design current of 10-18kA. A pulse coil will impose additional fields of 0.14T and 0.1T perpendicular and parallel to the conductor, respectively. The pulse loading will be ramped up in 1 sec. The TF coils will have simulated radiation heating of 0.1W/kg with selected local values reaching 0.5W/kg. Figure 1 illustrates a model of the six coil assembly placed around the central bucking post and resting on the spider base. The vacuum tank is not shown.

The test stand supports the entire weight of the facility. It also provides a high thermal resistance between the bucking post (at 5K) and the vacuum tank (at 80K). The central bucking post must resist a major portion of the TF coil centering and out of plane (overturning) forces. This is done through bearing surfaces and tongue-and-groove joints along the interface between the TF coil and bucking post. The two torque rings that clamp the outer corners of the test coils help resist overturning forces and are designed to allow the testing of from one to six coils in the test stand without the use of dummy coils.

Respective views, with hidden line removal, of finite element models of a TF coil case and the spider support base are given in Figs. 2 and 3, respectively. The base legs extend out between the TF coils and are pin supported at the ends. A half symmetric mesh of the bucking post cross section is shown in Fig. 4. The bucking post is a major structural component. It is basically a beam of hexagonal cross section. It has six cooling channels and a larger center void to reduce its weight and thermal capacity.

The loads applied to the bucking post are complex. There is a major radial centering force through the face of each coil. The pulsed fields tend to rotate (overturn) the coils about their horizontal midplane. If a single coil is energized it attempts to deform from a D shape to an O shape. Thus the bucking post is subjected to various combinations of compression, torsion, bending, gravity, and thermal loads.

The six toroidal field coils have different designs and come from different suppliers. However, they all satisfy certain interface conditions given in the design specification. Table I gives a summary of selected coil features.

LCTF Assembly Structural Analysis

The initial overall structural analysis of the Large Coil Test Facility (LCTF) was performed by Science Applications, Inc. (SAI). SAI employed the NASTRAN (8) program as well as a suite of specially developed pre- and postprocessors. Their NASTRAN model included beam element models of the bucking post, spider base, torque rings, and pulse coil system. The six TF coils and cases were modeled with beam and plate elements. A major goal of that study was to establish the interface displacement conditions that the six coils had to satisfy. Details of that study are given in Moses and Johnson (9).

The SAI assembly analysis did not consider local stress concentration such as holes, notches, etc. The coil conductor was assumed to resist hoop tension only. The surrounding steel case was modeled to carry the bending, torsion, and shear loads. Other beams, such as the bucking post, included the appropriate

TABLE I
LCP Test Coil Features

	GD/Convaair	GE	Westinghouse	EURATOM	Japan	Switzerland
Ampere	6.65×10^6	6.98×10^6	7.36×10^6	6.62×10^6	6.76×10^6	6.6×10^6
Conductor current	10,200 A	10,450 A	16,000 A	11,000 A	10,210 A	15,000 A
Conductor material	NbTi	NbTi	Nb ₃ Sn	NbTi	NbTi	NbTi
Structural material	304L stainless steel	316LN stainless steel	2219-T87 plates A286 bolts	Stainless steel similar to 316LN	304L stainless steel	Stainless steel similar to 316LN
Structure configuration	Fully welded case	Welded case and bolted closure	Grooved flat plates, bolted	Welded case with bolted or welded closure	Welded case with bolted side plate closure	Bolted case

area, shear factors, and bending and torsional inertia of the actual cross section.

LCTF Component Analysis

As the manufacturer's designs have progressed, the more recent analyses of individual structural components in the LCTF have been undertaken by ORNL. These studies have used the original NASTRAN models as well as the ORNL versions of the structural analysis codes GIFTS (10), SAP V (11), and PAFEC (12) and PIGS (13). Much of the three dimensional graphics, including hidden line removal, was done using the MOVIE.BYU (14) program and special interfaces such as GFTMOV (15). These programs have been used to establish more detailed descriptions of the base, torque rings, and bucking post. An enhanced system model is also under study.

Spider Base Analysis

The spider base consists of six haunched wide-flanged, ribbed beams that join in the center, as shown in Fig. 3. Each of the outer legs is attached to the vacuum tank bottom with pin connections. The base has one-twelfth geometric symmetry which is modeled as shown in the isometric view of Fig. 5. There is mesh refinement to account for bolts that penetrate the top surface to attach the bucking post.

Figure 6 shows a MOVIE.BYU presentation of the VonMises equivalent stress contours for the worst loading case. This led to the selection of a maximum plate thickness of 7.6 cm in this stainless steel component.

Bucking Post Analysis

The general loading conditions were described earlier. This component has been analyzed as a plane strain component, as a beam and membrane system, and as a three-dimensional solid. These models are still being refined. To illustrate one typical loading state Fig. 7 shows loads acting on the boundaries of a plane strain half-symmetry model that was shown in Fig. 4. The loads represent zero current in the right coil while the other five are at their design current. The worst state stresses reach about 210 MPa. Additional details for the bucking post and torque ring analyses are given by Baudry and Gray (16).

New Assembly Model

The knowledge and experience gained in the above analyses are being used to formulate a new LCTF assembly model. Currently included in the new model are the base, bucking post, two TF coils and upper and lower torque rings. This model refinement (see Fig. 8) was dictated by sensitive regions in the component models and engineering judgement. It represents an initial shakedown test (hopefully to be performed in late 1981) and models only two of the six coils. About 12500 independent degrees of freedom are included in the NASTRAN model. Figure 9 shows a deflected model looking from above the facility. The deflections result from a combined loading case with gravity, thermal, and electromagnetic body forces.

The model has been formulated in subsections representing each of the major components. This facilitates the incorporation of any modeling details that become apparent from the individual component analysis while providing a consistent basis for substructuring the model in the future. Six individual coil models are being formulated to represent the six independent coil designs. The complete LCTF assembly model will include ten primary substructures and about 20,000 degrees of freedom.

ENGINEERING TEST FACILITY

One of the next steps along the way to a practical magnetic fusion reactor is to advance the engineering state of the art to a level similar to the advances made in physics. The Engineering Test Facility (ETF) being designed at ORNL is one such project. It will also involve large superconducting coils. The structural analysis of ETF is still in the preliminary stages.

The previous LCP studies have raised questions about the best method to resist the overturning forces acting on the coils. Thus alternatives to the torque rings are being considered. A current study is investigating the use of toroidal shell segments, near the top and bottom of the coils, to resist the torque. A

single coil segment model being analyzed with PAFEC is shown in Fig. 10. The shell segments can be clearly seen. Of course, more detailed studies will be required to consider the effects of various equipment penetrations required in shell segments. This is just one example of the increasing sophistication developing in the rapid evolution of the structural analyses of large superconducting devices.

REFERENCES

- 1 F. C. Moon, "Introduction to Superconducting Structures," AMD, ASME Winter Annual Meeting, 1980.
- 2 C. T. Sun and W. H. Gray, "Theoretical and Experimental Determination of Mechanical Properties of Superconducting Coil Composites," 6th Symp. Eng. Prob. Fusion Research, IEEE Pub. 75CH1097-5-NPS, 1975, pp. 261-265.
- 3 T. Y. Chang, H. Suzuki and M. Reich, "A Finite Element Model for Elastic and Slip Responses of Fusion Magnets," Computer Technology in Fusion Energy Research, J. E. Akin, W. H. Gray (Eds.) ASME Pub. PVP-PB-031, 1978, pp. 67-85.
- 4 W. H. Gray and J. E. Akin, "Finite Element Stress Analysis of Orthotropic Solenoids," 7th Symp. Eng. Prob. Fusion Research, IEEE Pub. 77CH1267-4-NPS, 1977, pp. 851-853.
- 5 W. D. Cain and W. H. Gray, "On Maximum Attainable Magnetic Fields in Toroids and Solenoids Subject to Strain Limitations," 8th Symp. Eng. Prob. Fusion Research, 1979, to appear.
- 6 Y. M. Eyssa, et al., "Structures for Large Superconducting Energy Storage Solenoids," AMD, ASME Winter Annual Meeting, 1980.
- 7 N. E. Johnson, "The Determination of Electromagnetic Forces in Tokamak Magnets Using the TORMAC Computer Program," 7th Symp. Eng. Prob. Fusion Research, IEEE Pub. 77CH1267-4-NPS, 1977, pp. 1352-1356.
- 8 C. W. McCormick, (Ed.), "The NASTRAN User's Manual (Level 16.0)," NASA SP-222(01), May, 1974.
- 9 S. D. Moses and N. E. Johnson, "Analysis Techniques for Evaluating the Structural-Response of the Large Coil Test Facility," Computer Technology in Fusion Research, J. E. Akin and W. H. Gray (Eds.), ASME Pub. PVP-PB-031, 1978, pp. 25-44.
- 10 W. H. Gray, "System Software for the ORNL Version of GIFTS 4B," ORNL TM-7009, 1979.
- 11 "SAP V: A Structural Analysis Program for Static and Dynamic Response of Linear System," Univ. of So. Calif., L.A., 1977.
- 12 J. E. Akin, B. R. Dewey and R. D. Henshell, "PAFEC: Programs for Automatic Finite Element Calculations," in Structural Mechanics Software Series III, N. Perrone and W. Pilkey (Eds.), Univ. of Va. Press, 1980 (to appear).
- 13 R. D. Henshell, "PIGS: PAFEC Interactive Graphics Suite--User Guide," PAFEC Inc., Knoxville, TN, 1979.
- 14 H. Christiansen and M. Stephenson, "MOVIE.BYU: A General Purpose Computer Graphics Display System," Brigham Young Univ., 1978.
- 15 W. H. Gray, "A User's Guide to Program GFTMOV: A Computer Program to Access and Format a GIFTS 4B UDB into a Data Base for the MOVIE.BYU Program," ORNL TM-7021, 1979.
- 16 T. V. Baudry and W. H. Gray, "Using GIFTS on the CRAY-1 for the Large Coil Test Facility Test Stand Design Analysis, to appear.

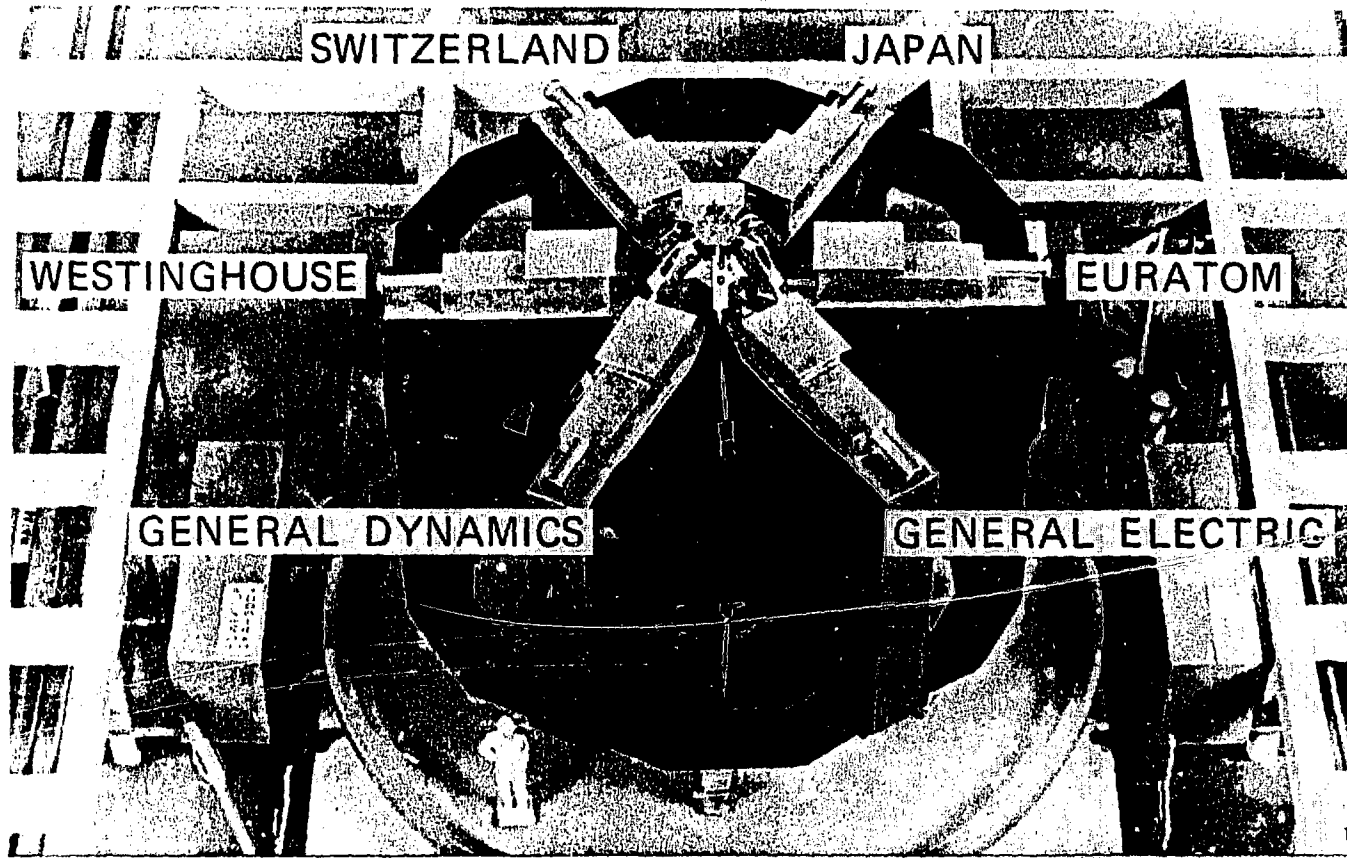


Fig. 1. A Model of the Assembled LCTF.

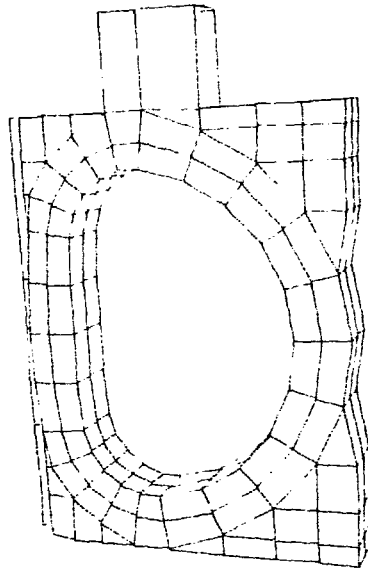


Fig. 2. A perspective view of the GD toroidal field coil finite element model for the new LCTF structural model. This view is of the left surface of the coil. (The hidden lines have been removed for clarity.)

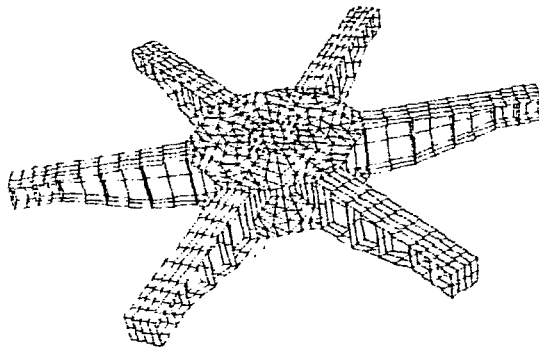


Fig. 3. A perspective view with the hidden lines removed of the LCTF spider base full finite element model. This model clearly presents the ribbed structure of the spider leg beams. (The observer's eye is located above the top surface of the spider base.)

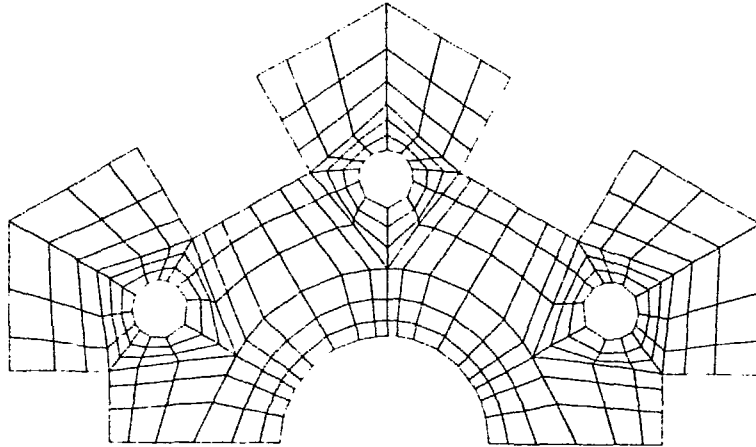


Fig. 4. A one-half symmetric plane strain finite element model of the LCTF bucking post. This cross section clearly shows the cooling channels and grooves for the toroidal field coils.

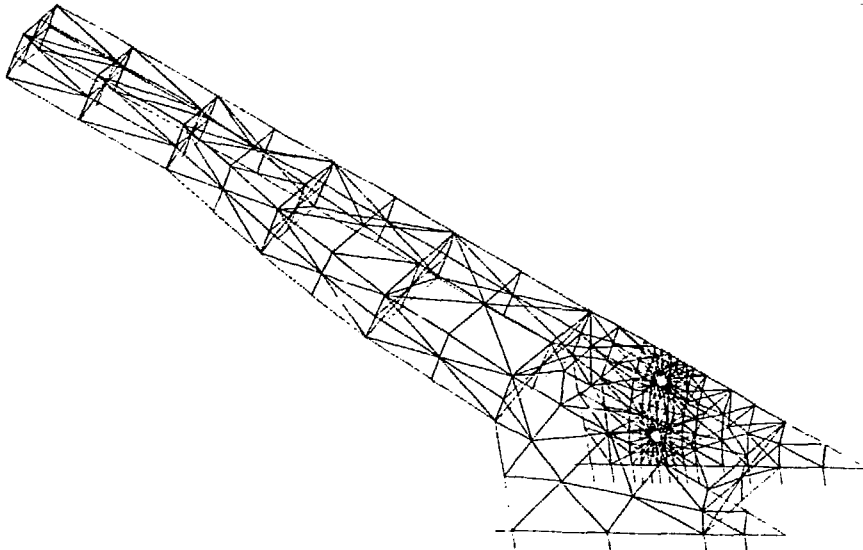


Fig. 5. An isometric view of the LCTF spider base, one-twelfth symmetric finite element model. This model was used to capture the mechanical response of the spider base's top plates, which are penetrated with bolt holes for the bucking post connection.

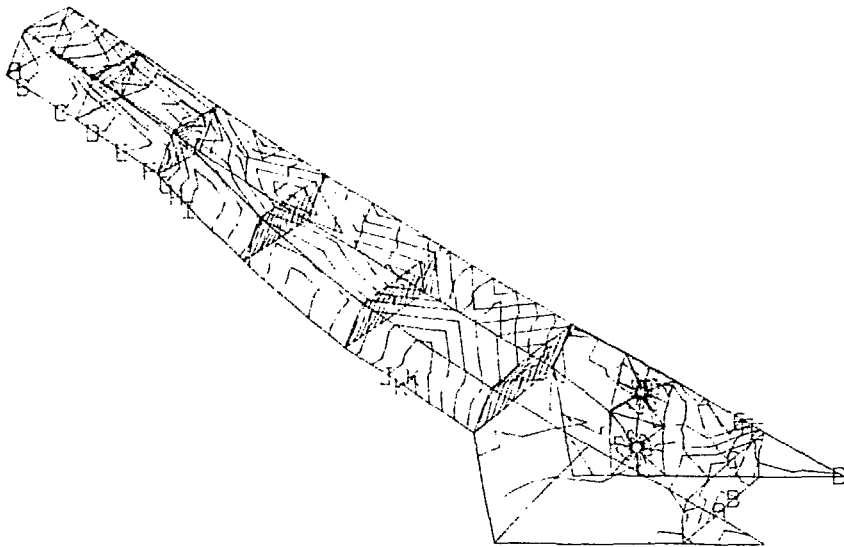


Fig. 6. An isometric view of the equivalent stress contours of the LCTF spider base finite element model. The highest stress contour is identified by the letter K and the other contours are linearly distributed between K and zero. As indicated by the analysis, the maximum plate thickness was increased on the top surface of the spider base. The maximum tensile stress now occurs on the bottom surface of the spider base.

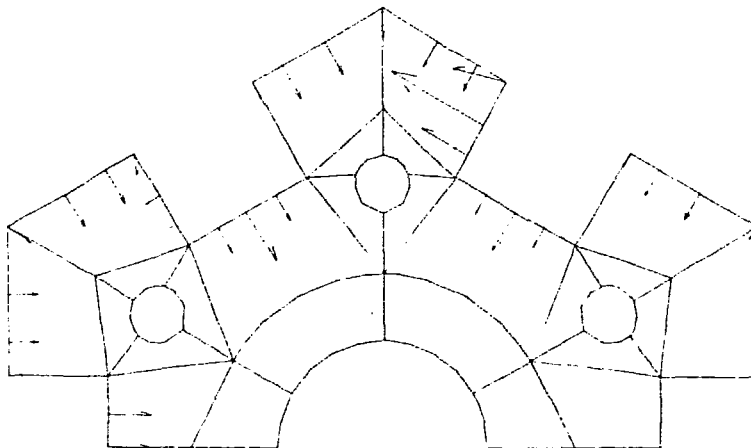


Fig. 7. A composite loading condition simulating zero current in the right-most coil while the other five coils are at design current. The loads are represented as vectors. (For clarity, only the boundary lines of the plane strain finite element model of the LCTF bucking post are drawn.)

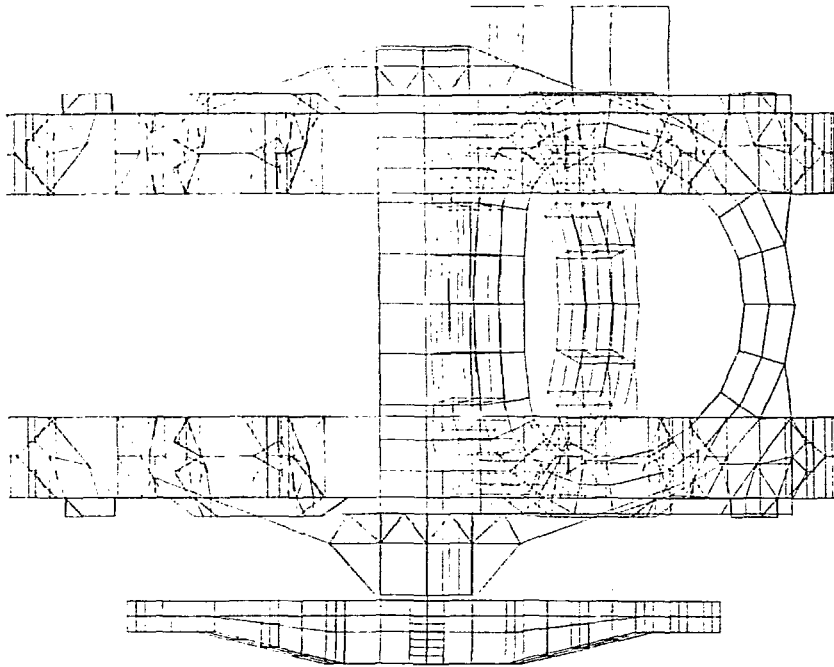


Fig. 8. An isometric view of the assembled LCTF structural model. All elements are shown. (The observer's eye is located directly in back of positive y axis.)

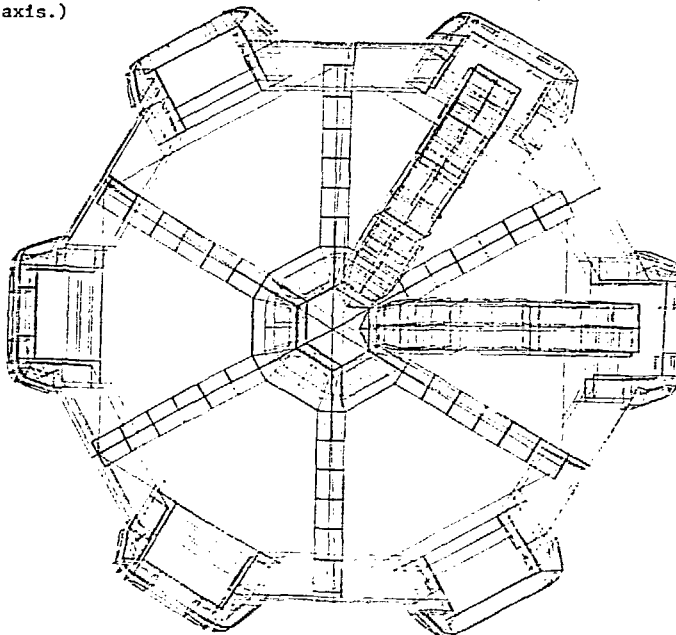


Fig. 9. An isometric view of the assembled LCTF structural model. Mechanical response due to the combined gravitation, thermal, and electromagnetic loads is shown using magnified deflections. The observer's eye is located directly above the facility.

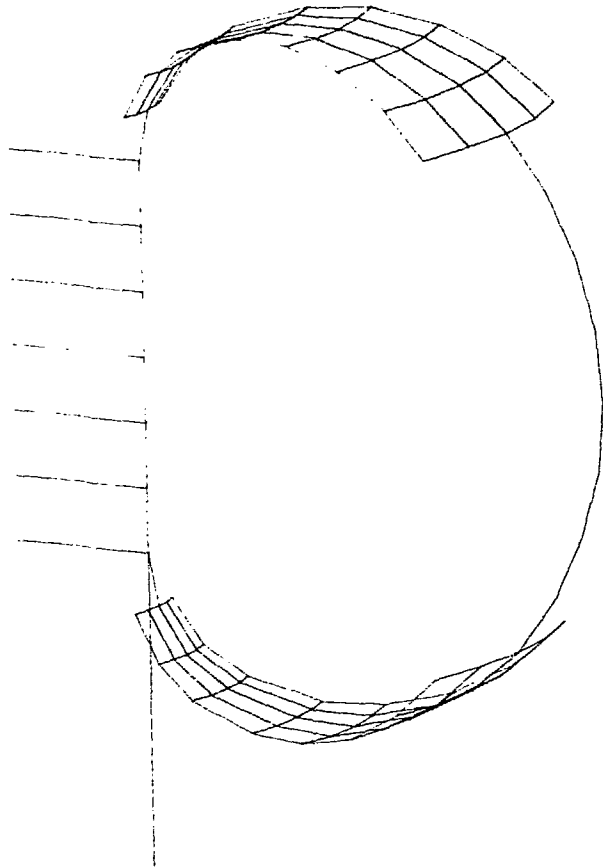


Fig. 10. An isometric view of the ETF one coil segment model.

